14th European Signal Processing Conference (EUSIPCO 2006), Florence, Italy, September 4-8, 2006, copyright by EURASIP

IMPROVING THE ACCURACY OF NOISE ESTIMATION WHEN USING DECISION FEEDBACK

Stefan Edinger[1]*, Markus Gaida*[2]*, and Norbert J. Fliege*[3]

Chair of Electrical Engineering, Faculty of Mathematics & Computer Science, University of Mannheim
University of Mannheim, 68131 Mannheim, Germany
phone: + (49) 621 181 3768, fax: + (49) 621 181 2682
email: {[1]stefan.edinger | [2]gaida | [3]fliege}@ti.uni-mannheim.de
web: et.ti.uni-mannheim.de

ABSTRACT

In discrete multitone transmissions, decision feedback is an attractive and simple method to gain information about transmission channel conditions without having to use pilot subcarriers or training sequences. Decision feedback, however, is prone to errors caused by wrong decisions. A misestimation of the true channel conditions often occurs when the signal-to-noise ratio is suddenly decreased by a disturbance. In this paper, we present novel measures to increase the overall accuracy of channel estimation. In particular, we identify a special statistic whose evaluation yields reliable noise estimates even for very low signal-to-noise ratios.

1. INTRODUCTION

Discrete multitone (DMT) transmission systems are characterized by a channel transfer function that is virtually constant over time. This allows for close adaptation of the transmission parameters to the individual transmission channel [1], [2]. At our chair, we are working on the design of DMT systems for industrial telecontrol applications [3],[4]. These applications require high reliability and great flexibility in data transmission over very long transmission lines.

Noise conditions for the considered transmission lines may be quickly changing. Narrowband interference can suddenly occur at any spectral location and vanish equally suddenly. Conventional DMT systems such as ADSL provide basic runtime adaptation capabilities such as bit-swapping and power adaptation [5]. Our DMT systems are especially designed to provide extensive dynamic adaptation strategies. The basic philosophy of dynamic adaptive DMT systems is that quick adaptation to changed channel conditions is more efficient than re-establishing a connection when it has broken [6]. During the short adaptation phase, an increase of error rates is acceptable. Higher level protocols can usually cope with such short error bursts, e.g. by requesting a retransmission of defective data. Therefore, error detection and correction functionality is kept to a minimum in our systems to provide as much bandwidth for data transmission as possible.

When the signal-to-noise ratio (SNR) of the transmission channel suddenly deteriorates, the required bit error rates (BER) usually can not be maintained any more. Instead of trying to restore acceptable data rates by using basic adaptation strategies which are likely to fail, we continue to transmit data over heavily disturbed subcarriers. The advanced noise estimation techniques presented in this paper allow us to quickly gain accurate information about the disturbance. As soon as noise powers are estimated sufficiently reliably, adapted transmission parameters that take into account the changed channel conditions can be computed and take effect.

This work was partly funded by the German Research Foundation (Deutsche Forschungsgemeinschaft, DFG)

2. SYSTEM DESIGN

The system design of our transceivers is depicted in Fig. 1. We will first describe how the system initially adapts itself to the individual channel it is confronted with and then outline the flow of information during regular data transmission.

2.1 Initial Adaptation

Before actual data transmission can start, information about the transmission channel, its transfer function and noise conditions must be gathered. To this end, a pseudo random noise sequence known to both transceivers is transmitted and evaluated. After this estimation phase, both the channel transfer function H_c and noise powers N_i for each subcarrier i are known. Let P_{ref} denote the so-called reference power that is equal for all subcarriers during transmission of the estimation sequence. P_{ref} is derived by distributing the limited total transmit power P_{tot} equally over all subcarriers. Signal-to-noise ratios for each subcarrier i can then be computed by $SNR_i = \frac{g_i \cdot P_{ref}}{N_i}$, where g_i denotes the attenuation caused by the transmission channel at subcarrier i.

The SNR_i serve as input for a so-called rate-maximizing bit loading algorithm (e.g. [7]). This algorithm maximizes the number of bits that can be transmitted at a given bit error rate (BER) over the transmission channel without exceeding the transmit power limit P_{tot}. Its output are a bit allocation table (BAT) that indicates how many bits should be transmitted per subcarrier and a power allocation table (PAT) that indicates what transmit power should be used for each subcarrier to meet the desired BER.

BAT and PAT are the most important transmission parameters for DMT systems. Additionally, the frequency domain equalizer (FEQ) that removes distortions caused by the channel is initialized using information gathered about H_c.

2.2 Regular Data Transmission

After the transmission parameters are initialized, actual data transmission can start. Our system uses a sampling frequency of 1024 kHz. Blocks of binary input data are first converted serial-to-parallel (S/P). The parallel data is distributed onto the individual subcarriers according to the BAT and modulated using quadrature amplitude modulation (QAM). Only equispaced square constellations are used, thus only even

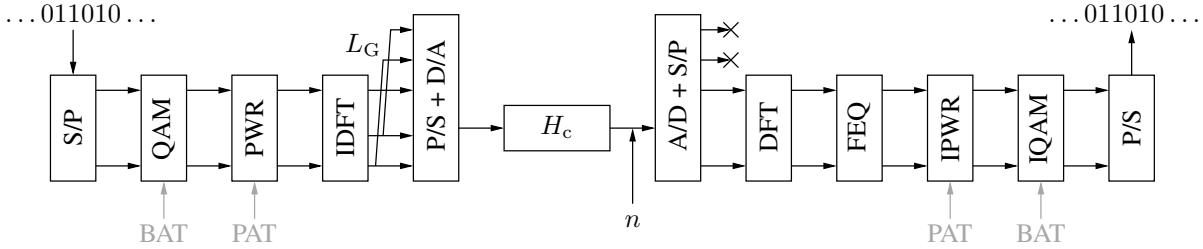

Figure 1: Schematic system model

numbers b_i of bits per subcarrier i can be transmitted and we limit this number to $b_i \leq 12$ for performance reasons.

After QAM, the mean power p_i for each modulated subcarrier is normalized to $p_i = 1$. Each subcarrier is subsequently power-scaled according to the PAT to meet the specific BER requirements. The time domain signal is generated using an inverse discrete Fourier transformation with length $M = 128$. Transmission takes place in the baseband, thus only $M/2 = 64$ subcarriers can be modulated independently. A cyclic prefix (guard interval) of $L_G = 32$ is used to prevent intersymbol and intercarrier interference (ISI and ICI). We assume that L_G is at least as long as the channel impulse response. We thus do not need to consider influences of ISI and ICI. In the time domain, one DMT symbol consists of $128 + 32 = 160$ samples and the transmission rate equals 6400 DMT symbols per second.

The DMT symbol is transmitted over the channel with transfer function H_c and corrupted by additive noise n (both white Gaussian noise (AWGN) and narrowband interference can be considered). At the receiver, the cyclic prefix is removed and the DMT symbol is converted to the frequency domain using the discrete Fourier transform of length M. Both IDFT and DFT are efficiently implemented as fast Fourier transforms (FFT). Distortions caused by the transmission channel are reversed in the frequency domain equalizer (FEQ) which is implemented as a one-tap equalizer. Power-scaling according to the PAT is reversed and the received QAM symbols are demodulated in the inverse QAM block (IQAM). Additive noise power increases the mean power at the receiver, thus values $p_i \geq 1$ are to be expected. After a final P/S conversion, the original binary data sequence is restored.

3. DECISION FEEDBACK AND MISESTIMATION

During regular data transmission, noise conditions are monitored. Consider Fig. 2, which shows a 16-QAM constellation with decision regions. Suppose complex signal point q_1 was transmitted. Noise corrupts the transmitted signal and the receiver receives, say, signal point r. The exact noise vector e can be computed as $e = r - q_1$. The receiver maps or decides the signal point r to the most likely transmit symbol. We use a ML (maximum likelihood) receiver that maps a received signal point r to point q_1 whenever r lies within the square decision region of q, delimited by the dashed lines. The decided (or estimated) signal is denoted by $\hat{q}$ in the following. From this estimate, the noise estimate is computed as $\hat{e} = \hat{q} - r$. If the exact noise vector e does not move the received signal point out of the transmitted signal point's decision region, the decision is correct and the noise estimate is correct as well, thus $\hat{e} = e$.

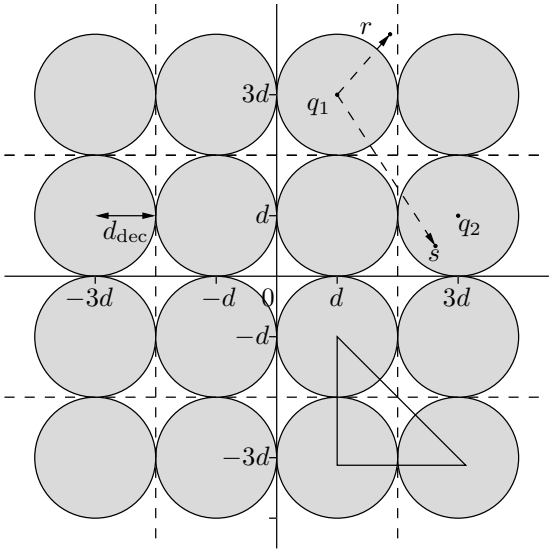

Figure 2: Decision regions for 16-QAM

Now consider the case that q_1 was transmitted but signal point s was received. The decided signal point $\hat{q} = q_2$. Clearly, a wrong decision is made. While the exact noise vector is $e = q_1 - s$, the estimated noise vector is $\hat{e} = \hat{q} - s = q_2 - s$. Noise is underestimated. Specifically, $\hat{e} < d_{\text{dec}}$, where d_{dec} denotes the decision boundary for the 16-QAM constellation and here, $d_{\text{dec}} = d$. The mean signal energy E for square equispaced N-QAM constellations, where $N = 2^{b_i}$ and signal points are spaced $2d$ apart from each other, can be computed as

$$E = d^2 \cdot \frac{2(N-1)}{3}. \tag{1}$$

Since E is normalized to $E = 1$ after QAM and before IQAM, d can be computed as

$$d = \sqrt{\frac{3 \cdot 1}{2\,(N-1)}}. \tag{2}$$

If a noise vector exceeds d_{dec} in quadrature or in-phase axis, a wrong decision is made, except the noise vector moves the signal point favorably outside the outer border of the constellation.

The gray shaded circles in Fig. 2 mark areas where received signal points will yield error estimates $|\hat{e}| \leq d_{\text{dec}}$, regardless of which signal point was transmitted. White regions mark areas where $|\hat{e}| > d_{\text{dec}}$.

Decision feedback (DF) relies on the decided signal points to estimate the mean noise power $\overline{|\hat{e}|^2}$ and SNR. Wrong decisions lead to an underestimation of the actual noise power. Error correcting codes such as Reed Solomon codes can be used to detect and correct wrong decisions and thus be able to infer the correct noise vector e. However, as mentioned previously, we do not use any coding techniques to keep the transceiver structure as simple as possible and instead rely on higher level protocols to provide error detection or correction capability.

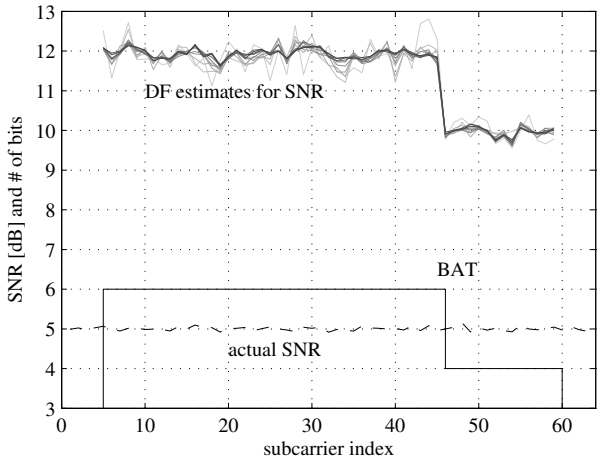

Figure 3: Underestimation of noise due to DF

Fig. 3 shows the phenomenon of noise underestimation caused by wrong decisions in DF. To concentrate on the effects of interest, we start by considering an ideal channel ($g_i = 1$ for all i) with only AWGN. The original SNR present at the time of initial adaptation was 25 dB. If due to a disturbance the actual SNR drops to only 5 dB, this new SNR is not estimated correctly. A number of estimates computed by using consecutively more sample values are shown (starting from 500 samples up to 5000 samples). Estimates using fewer sample values are shown in lighter gray.

It is evident that increasing the observation period and considering more sample values does not increase the accuracy of the noise estimation. Also shown in the figure is the BAT. A given noise power has less impact for smaller constellation sizes. Nevertheless, noise is underestimated by at least 5 dB. If adaptation were based on the depicted estimation values, severe degradation of BER would have to be expected.

4. IMPROVING THE ACCURACY OF DF ESTIMATION

Let n_{le} denote the number of noise samples with $|\hat{e}| \leq d_{\text{dec}}$ and n_{gt} denote the number of noise samples with $|\hat{e}| > d_{\text{dec}}$. The ratio

$$R = \frac{n_{\text{gt}}}{n_{\text{le}} + n_{\text{gt}}} \tag{3}$$

can be used to significantly improve the accuracy of noise power estimation.

4.1 Empiric Results

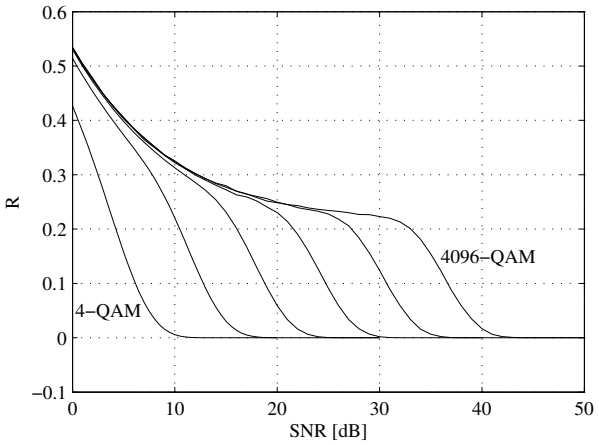

Figure 4: R for various constellations and SNR values

Using simulation results, Fig. 4 shows the ratio R for different constellation sizes (N-QAM from $N = 4$ up to $N = 4096$) and different SNR values. Note that mean signal power is normalized to $E = 1$ for all constellations. Thus, the respective noise powers are just the inverse in linear scale.

In the following section we will derive an exact formula to give the ratio R. Numerical integration methods can then be used to compute R for arbitrary constellations and noise powers. Comparison of simulation results and numerical evaluation of the theoretical results has shown excellent agreement.

4.2 Theoretical Derivation

A two-dimensional Gaussian for vector $\mathbf{x} = (x_1, x_2)^T$ and mean $\overline{\mathbf{x}} = (\overline{x_1}, \overline{x_2})^T$ is given by [8]

$$P(\mathbf{x}) = \frac{1}{\sqrt{(2\pi)^2 |\mathbf{V}|}} \exp\left[-\frac{1}{2} (\mathbf{x} - \overline{\mathbf{x}})^T \mathbf{V}^{-1} (\mathbf{x} - \overline{\mathbf{x}}) \right], \tag{4}$$

where the variance-covariance matrix $\mathbf{V}$ is

$$\mathbf{V} = \begin{pmatrix} \sigma_1^2 & \sigma_{12}^2 \\ \sigma_{21}^2 & \sigma_2^2 \end{pmatrix}. \tag{5}$$

Since the statistics of both in-phase and quadrature component are uncorrelated, $\mathbf{V}$ becomes a diagonal matrix. Thus, inversion and determinant of $\mathbf{V}$ are trivial to compute. Additionally, in our case $\sigma_1^2 = \sigma_2^2 = \sigma^2$.

With $\mathbf{x} = (x_1, x_2)^T$, where x_1 and x_2 denote in-phase and quadrature component of the vector, and some simplifications, Eq. (4) can be rewritten as

$$P(x_1, x_2) = \frac{1}{2\pi\sigma^2} \exp\left(-\frac{(x_1 - \overline{x_1})^2 + (x_2 - \overline{x_2})^2}{2\sigma^2} \right). \tag{6}$$

Note that the variance of the two-dimensional Gaussian, σ_{2D}^2 is split into an in-phase and quadrature component, thus $\sigma^2 = \frac{\sigma_{2D}^2}{2}$.

For the constellation from Fig. 2, an exemplary two-dimensional Gaussian centered at one of the inner constellation points and evaluated over the gray-shaded circles in Fig. 2 is depicted in Fig. 5.

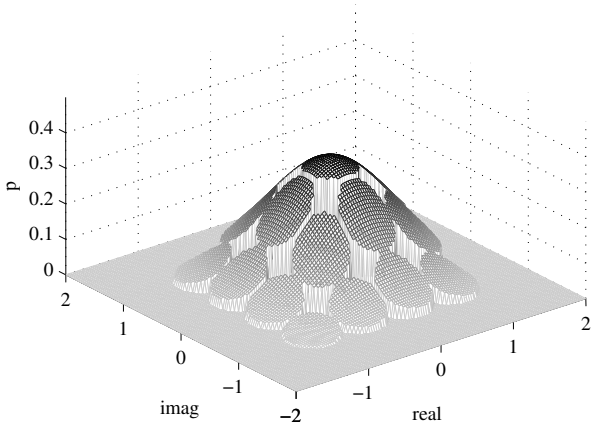

Figure 5: Plot of two-dimensional Gaussian

The probability P_{le} that $|\hat{e}| \leq d_{\text{dec}}$ is just the volume above all circles which can be computed by evaluating the two-dimensional integral over Eq. (6) for each circle and summing up the results for all transmit constellation points and circles like this:

$$P_{\text{le}} = \sum_{x_1 \in D} \sum_{x_2 \in D} \sum_{x_1^c \in D} \sum_{x_2^c \in D} \int_A P(x_1, x_2)\, dx_1 dx_2 \,. \qquad (7)$$

In Eq. (7), the set D contains all coordinates for constellation points, e.g. for the 16-QAM $D = \{-3d, -d, d, 3d\}$ and the integration area A is defined as

$$A = (x_1 - x_1^c)^2 + (x_2 - x_2^c)^2 \leq d_{\text{dec}}^2 \,, \qquad (8)$$

the area of a circle with radius d_{dec} and center (x_1^c, x_2^c).

In practice, the evaluation of the above formula can be sped up by noting that not all constellation points need to be considered in the two outermost sums. Due to the symmetry of square constellations, only about one eighth of the constellation points (one half quadrant including the diagonal, for example for a 16-QAM the points covered by the triangle in Fig. 2) need to be considered. The results must then be weighted appropriately.

R from Eq. (3) can now be computed as

$$R = 1 - P_{\text{le}} \,. \qquad (9)$$

4.3 Practical Considerations

To use the ratio R to improve the DF estimation of SNR and noise powers, one must compute the inverse of the curves shown in Fig. 4. For practical reasons, we evaluated R for a number of SNR values and derived interpolating curves for functions SNR_{est} that depend on N and R. We used both rational functions and polynomials depending on which yielded the best fit. Clearly, some error is made using interpolating curves, but they enable fast computation of SNR estimates given a specific R.

5. SIMULATION RESULTS

Using the interpolating functions $\text{SNR}_{\text{est}}(\text{R},\text{N})$ derived above, we simulated the same transmission as in the previous example shown in Fig. 3. Results are depicted in Fig. 6. The actual SNR is again 5 dB. The improved estimate comes much closer than the original estimates using pure DF. To fit the parameter R into the same figure, its value, multiplied by 10 is depicted. It can be seen that smaller constellation sizes yield larger R for the same noise power, because their transmit power is smaller.

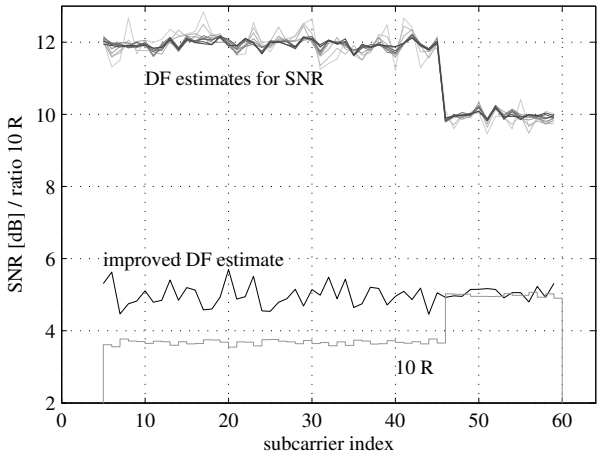

Figure 6: Increased accuracy of DF estimation

The deviations from the correct SNR value of 5 dB are due to sensitivities of the characteristic curves for some ranges of input values and interpolation deviations. At additional computational and hardware complexity, the accuracy could be improved further. Even without additional measures, however, the improved estimation comes very close to the correct SNR value. Adaptation based on these improved estimates will yield acceptable if not excellent BER performance.

5.1 Extension to General Channel Model

To focus on the relevant parameters, we have so far only considered a flat channel with AWGN. The proposed estimation method works equally satisfyingly for general channels with realistic transfer functions and narrowband interference.

We consider a narrowband interference having a bandwidth smaller than one subcarrier spacing and center frequency exactly between subcarriers 10 and 11. Due to the leakage effect of the DFT, not only directly affected subcarriers are disturbed but noise power leaks into adjacent subcarriers, and even subcarriers further away from the center frequency of the interference experience significant amounts of noise power.

Fig. 7 shows both the original SNR used for bit loading and the actual SNR caused by the interference. The gray lines represent estimates derived by pure DF. As before, wrong decisions lead to misestimation of the true noise power. The improved DF estimate, however, comes very close to the true SNR.

Finally, Fig. 8 shows an improved DF estimation for a realistic channel and only AWGN. Noise power is raised by

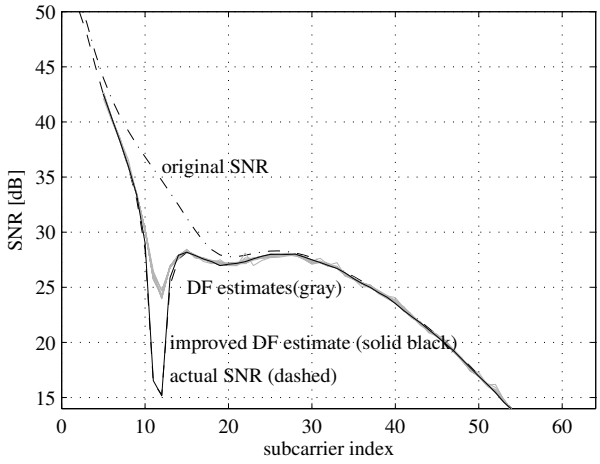

Figure 7: Improved DF estimation for narrowband interference

20 dB. As expected, the improved DF estimation performs much better than pure DF estimation.

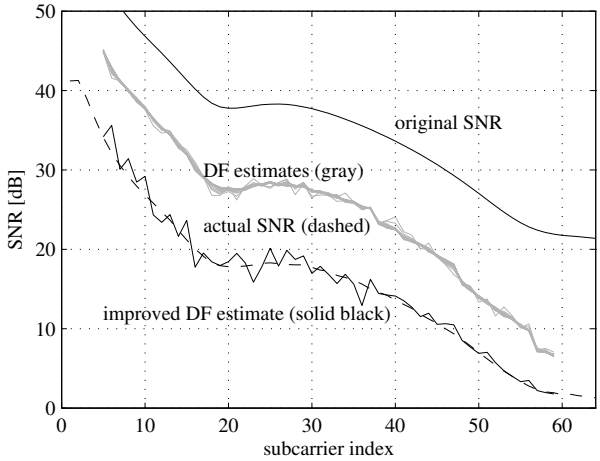

Figure 8: Improved DF estimation for AWGN only

5.2 Further Improvements

In the previous figure, the improved DF estimate exhibited rather strong variance. If only AWGN is encountered, one can greatly enhance the estimate if one computes the mean noise power over all used subcarriers. It is relatively easy to determine whether AWGN or narrowband interference is present by comparing noise differences on individual subcarriers. For narrowband interference, smoothing would yield defective results.

Fig. 9 shows the same simulation parameters as Fig. 8. This time, though, the noise power was averaged over all used subcarriers. This levels out variances that occur for various reasons from subcarrier to subcarrier. The resulting improved DF estimate is very smooth and provides an excellent fit of the actual SNR.

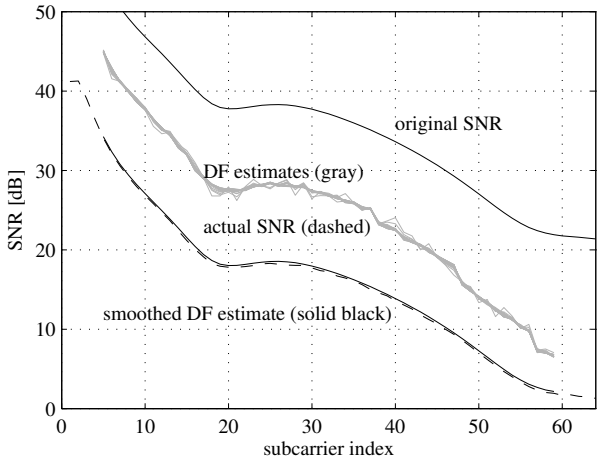

Figure 9: Smoothed improved DF estimation

6. CONCLUSION

We presented a novel method to increase the accuracy of SNR and noise estimation using decision feedback. We justified our choice to not use low-level error detection or control and instead to rely on higher level protocols to provide the respective functionality. If such functionality is given, our methods provide an easy-to-implement, reliable and fast way to gather accurate information about changed noise conditions. This information is then used to compute adapted transmission parameters which will restore the required quality of transmission.

REFERENCES

[1] Thomas Starr, John M. Cioffi, and Peter J. Silverman. *Understanding Digital Subscriber Line Technology*. Prentice Hall, 1999.

[2] John A. C. Bingham. *ADSL, VDSL, and Multicarrier Modulation*. Wiley, 1999.

[3] Carsten Bauer. *Mehrträger-Übertragungssysteme mit dynamischer Adaption an zeitvariante Kanaleigenschaften*. Dissertation, Universität Mannheim, 2004.

[4] Stefan Edinger, Carsten Bauer, and Norbert J. Fliege. DMT Transmission in the Context of Industrial Telecontrol Applications. In *Kleinheubacher Tagung*, Miltenberg, Germany, September 2005.

[5] L. Hoo, A. Salvekar, C. Aldana, J. M. Cioffi, P. Chow, and J. Carlo. Express and Confirmation AOC Swapping Commands for DMT DSLs. *ANSI Contribution T1E1.4/99-118*, March 1999.

[6] Stefan Edinger and Carsten Bauer. Concepts of Dynamic Adaptive DMT Modulation. In *ISCCSP*, Marrakech, Morocco, March 2006.

[7] Dirk Hughes-Hartogs. *Ensemble Modem Structure for Imperfect Transmission Media*. U.S. Patents No. 4679227 (July 1987), 4731816 (March 1988), 4833706 (May 1989), 1989.

[8] Kristian Kroschel. *Statistische Informationstechnik*. Springer-Verlag, 4. edition, 2004.